

Supporting Information

Transition-Metal-Free Highly Chemo- and Regioselective Arylation of Unactivated Arenes with Aryl Halides over Recyclable Heterogeneous Catalysts

Hongli Liu, Biaolin Yin, Zhiqiang Gao, Yingwei Li,* and Huanfeng Jiang*

*School of Chemistry and Chemical Engineering, South China University of Technology, Guangzhou
510640, China.*

E-mail: liyw@scut.edu.cn

Table of Contents

General Information	SI-2
Experimental Section	SI-2
Catalyst characterization and reaction results (Tables S1-S4 and Figures S1-S5)	SI-5
Spectra Data for the Products	SI-14
¹ H NMR and ¹³ C NMR Spectra of products	SI-18

1. General Information

Aryl halides and bases were purchased from commercial sources and used without further treatments. All solvents were analytical grade and distilled prior to use.

^1H NMR and ^{13}C NMR data were obtained on Bruker Avance III 400 spectrometer using CDCl_3 as solvent and tetramethylsilane (TMS) as an internal standard. Mass spectra were recorded on a GC-MS spectrometer (Shimadzu GCMS-QP5050A equipped with a $0.25\text{ mm} \times 30\text{ m}$ DB-WAX capillary column). Powder X-ray diffraction patterns of the samples were obtained on a Rigaku diffractometer (D/MAX-III A, 3 kW) using $\text{Cu K}\alpha$ radiation (40 kV, 30 mA, $\lambda = 0.1543\text{ nm}$). BET surface area and pore size measurements were performed with N_2 adsorption/desorption isotherms at 77 K on a Micromeritics ASAP 2020 instrument.

2. Experimental Section

2.1 Synthesis of MOF-253¹

MOF-253 was prepared from hydrothermal reaction of $\text{AlCl}_3 \cdot 6\text{H}_2\text{O}$ (151 mg, 0.625 mmol), glacial acetic acid (859 μL , 15.0 mmol), 2,2'-bipyridine-5,5'-dicarboxylic acid (153 mg, 0.625 mmol), and 10 mL $\text{N,N}'$ -dimethylformamide (DMF) at 120 °C for 24 h. The resulting white microcrystalline powder was then filtered and washed with DMF. The solid was washed with methanol via soxhlet extraction for 24 h, and then was collected by filtration and finally dried at 250 °C under vacuum for 12 h. Anal. Calcd for $\text{C}_{12}\text{H}_7\text{AlN}_2\text{O}_5 \cdot 0.5\text{H}_2\text{O}$: Al, 9.14; C, 48.82; H, 2.74; N, 9.49. Found: Al, 8.80; C, 49.02; H, 2.53; N, 9.60.

2.2 General procedure for the direct arylation of benzene with aryl iodides

Aryl iodide (0.5 mmol, if solid), MOF-253 (0.15 mmol, 30 mol%), and $\text{KO}t\text{-Bu}$ (1.5 mmol, 3.0 equiv) were added to a Schlenk tube under a nitrogen atmosphere at room temperature. Benzene (4 mL) and aryl iodide (0.5 mmol, if liquid) were then added using a syringe. The tube was sealed and the mixture was stirred at the desired temperature. After cooling to room temperature, the solid catalyst was isolated from the solution by filtration and washed with ethyl acetate. The solution was filtered through a short plug of silica gel, and then washed with copious quantities of ethyl acetate. The combined organic

phase was concentrated under vacuum. The crude was purified by silica gel chromatography using petroleum ether/ethyl acetate as eluent to afford the desired product.

2.3 General procedure for the direct arylation of benzene with aryl bromides

Aryl bromide (0.5 mmol, if solid), MOF-253 (0.15 mmol, 30 mol%), and KO*t*-Bu (1.5 mmol, 3.0 equiv) were added to a Schlenk tube under a nitrogen atmosphere at room temperature. Benzene (4 mL) and aryl bromide (0.5 mmol, if liquid) were then added using a syringe. The tube was sealed and the mixture was stirred at the desired temperature. After cooling to room temperature, the solid catalyst was isolated from the solution by filtration and washed with ethyl acetate. The solution was filtered through a short plug of silica gel, and then washed with copious quantities of ethyl acetate. The combined organic phase was concentrated under vacuum. The crude was purified by silica gel chromatography using petroleum ether/ethyl acetate as eluent to afford the desired product.

2.4 General procedure for the direct arylation of arenes with 4-iodoanisole

4-Iodoanisole (0.5 mmol), MOF-253 (0.15 mmol, 30 mol%), KO*t*-Bu (1.5 mmol, 3.0 equiv), and arene (45 mmol, 90 equiv, if solid) were added to a Schlenk tube under a nitrogen atmosphere at room temperature. Arene (4 mL, if liquid) was then added using a syringe. The tube was sealed and the mixture was stirred at the desired temperature. Solid arene (e.g., naphthalene, M.P. = 80 °C) fully melted at the reaction temperature investigated. After cooling to room temperature, the solid catalyst was isolated from the solution by filtration and washed with ethyl acetate. The solution was filtered through a short plug of silica gel, and then washed with copious quantities of ethyl acetate. The combined organic phase was concentrated under vacuum. The crude was purified by silica gel chromatography using petroleum ether/ethyl acetate as eluent to afford the desired product.

2.5 Recycling of the MOF-253 catalyst

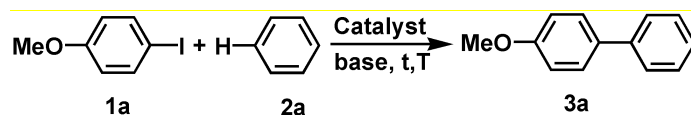
The recyclability of the MOF-253 catalyst was tested for direct arylation of benzene with 4-iodoanisole maintaining the same reaction conditions as described above, except using the recovered catalyst. The results of five runs are presented in Table S3. Each time, the reaction mixture was allowed to settle down at the end of catalytic reaction and the supernatant liquid was decanted. The solid was

thoroughly washed with benzene, dried, and then reused as catalyst in the next run. As shown in Table S2, the catalyst can be reused in the cross-coupling reaction five times without any significant loss of efficiency. The crystalline structure of the MOF-253 mostly remained unchanged after five runs of catalysis (Figure S2), confirming the stability of the MOF under the investigated conditions.

2.6 Heterogeneity of the catalyst

To verify whether the catalysis of MOF-253 is truly heterogeneous, the solid catalyst was hot filtered from the solution at ca. 20% conversion by a simple filtration. The reaction was continued with the filtrate for an additional 34 h. The solution in the absence of solid did not exhibit any further reactivity. The results demonstrate that the reaction proceeds on the heterogeneous surface.

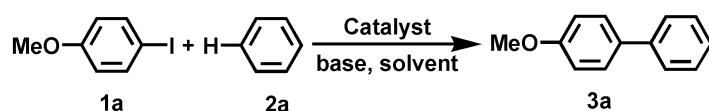
Table S1 Cross-coupling of benzene with 4-iodoanisole: screening of reaction conditions^a



Entry	Cat (mol %)	Base (equiv)	T (°C)	Conv (%) ^b	Yield (%) ^b
1	MOF-253 (20)	CH ₃ ONa(2)	100	—	—
2	MOF-253 (20)	NaOH (2)	100	—	—
3	MOF-253 (20)	KOH (2)	100	< 1	< 1
4	MOF-253 (20)	LiO <i>t</i> -Bu (2)	100	—	—
5	MOF-253 (20)	DABCO (2)	100	—	—
6	MOF-253 (20)	KO<i>t</i>-Bu (2)	100	50	50
7	—	KO <i>t</i> -Bu (2)	100	—	—
8	MOF-253 (20)	—	100	—	—
9	—	—	100	—	—
10	MOF-253 (20)	KO <i>t</i> -Bu (2)	80	34	34
11	MOF-253 (20)	KO <i>t</i> -Bu (2)	120	69	69
12	MOF-253 (20)	KO <i>t</i> -Bu (3)	100	72	72
13	MOF-253 (30)	KO <i>t</i> -Bu (2)	100	70	70
14	MOF-253 (30)	KO<i>t</i>-Bu (3)	100	87	87

^a Reaction conditions: **1a** (0.5 mmol), benzene (4 mL), 24 h. ^b Yields were determined by GC-MS analysis.

Table S2 Arylation of benzene with 4-iodoanisole in different solvents^a



Entry	Solvent	T (°C)	Time (h)	Yield (%) ^b
1	DMF	100	36	< 1
2	DMA	100	36	—
3	NMP	100	36	10
4	1,4-dioxane	100	36	35
5	acetonitrile	100	36	< 1
6	THF	100	36	25
7	1,4-dioxane	120	48	60

^a Reaction conditions: **1a** (0.5 mmol), benzene (20 mmol), KO*t*-Bu (3 equiv), MOF-253 (30 mol%), solvent (2 mL). ^b Determined by GC-MS.

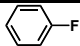
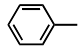

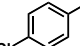
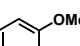
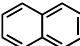
Table S3 Reusability of the MOF-253 catalyst in the cross-coupling of 4-iodoanisole with benzene.^a

Use	1st	2nd	3rd	4th	5th
Conv. (%) ^b	> 99	97	95	96	98
Sel. (%) ^b	> 99	> 99	> 99	> 99	> 99

^a Reaction conditions: 4-iodoanisole (0.5 mmol), KO^t-Bu (3 equiv), MOF-253 (30 mol%), benzene (4 mL), 100 °C, 36 h. ^b

Determined by GC-MS.

Table S4 Molecular x, and y dimensions of the arenes.

Molecule	x (Å)	y (Å)
	6.6	7.7
	6.6 ^a	8.2 ^a
	6.6	8.5
	6.6	8.8
	6.6	9.4
	7.3	9.5

^a C. E. Webster, R. S. Drago, M. C. Zerner, *J. Am Chem. Soc.* 1998, **120**, 5509.

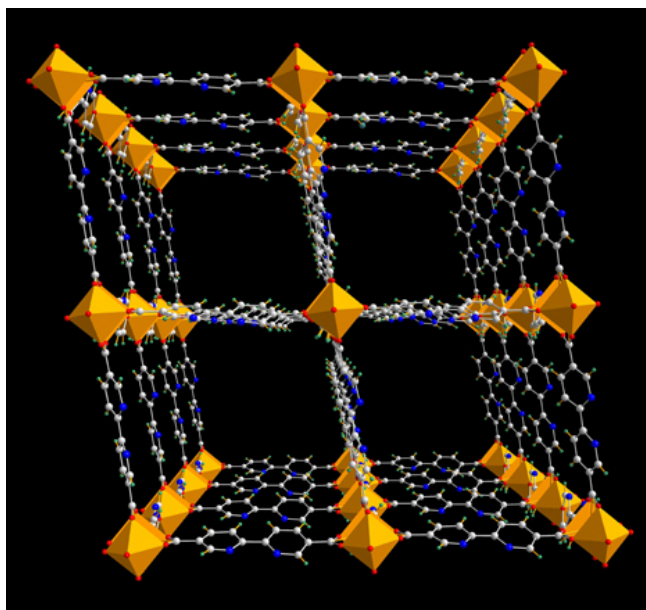


Figure S1. Representative structure of MOF-253. The orange octahedral represent the Al atoms. Oxygen, red; nitrogen, blue; carbon, gray; hydrogen, green.

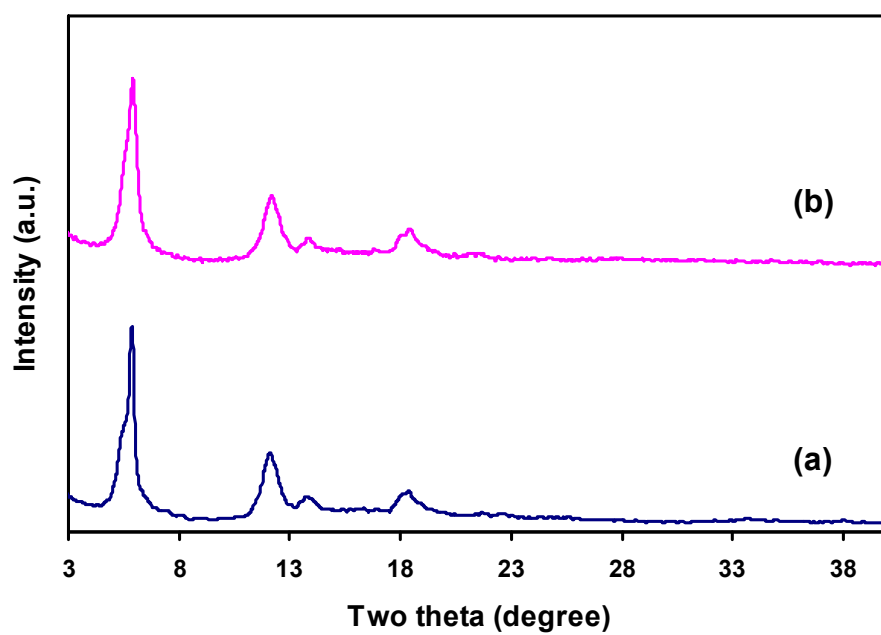


Figure S2. Powder XRD patterns for MOF-253 samples recorded before (a) and after catalytic reaction (b).

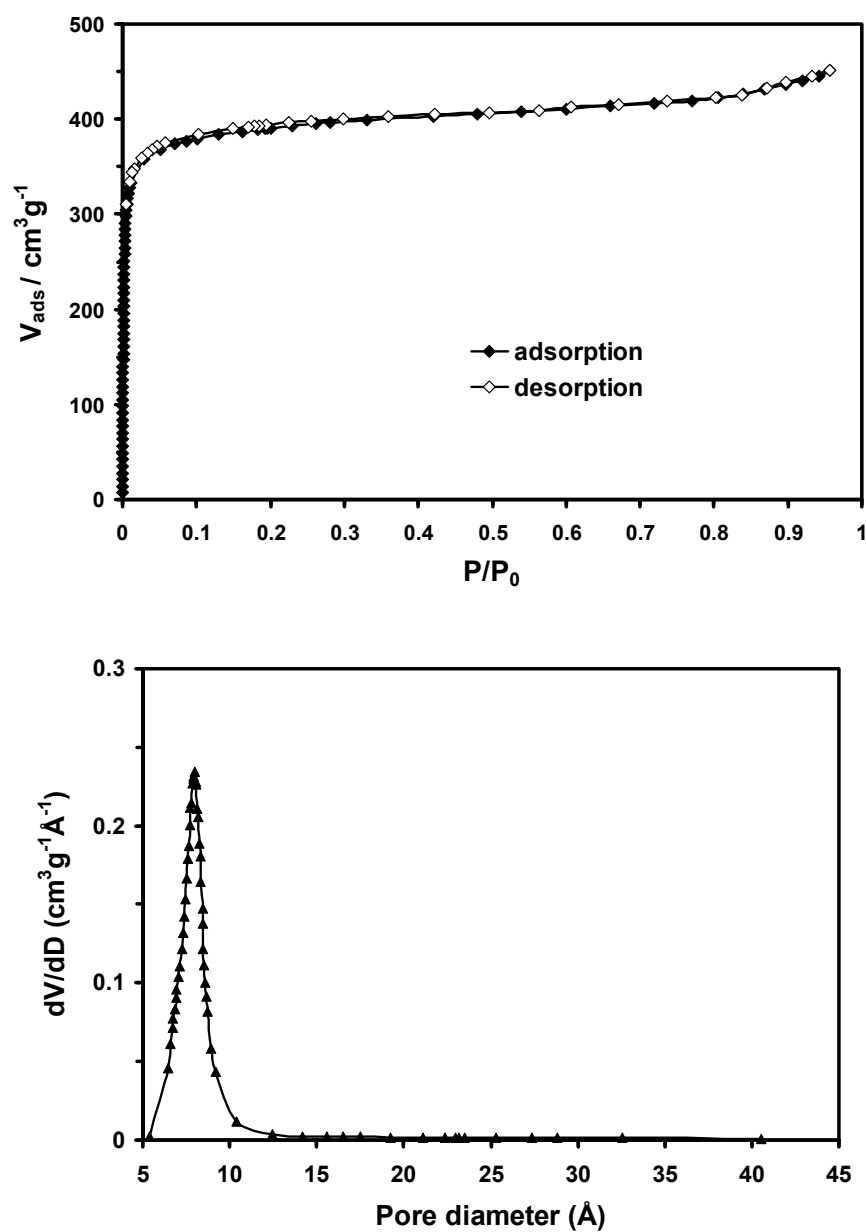


Figure S3. Nitrogen isotherms at 77 K (top) and micropore size distribution (bottom) of MOF-253.

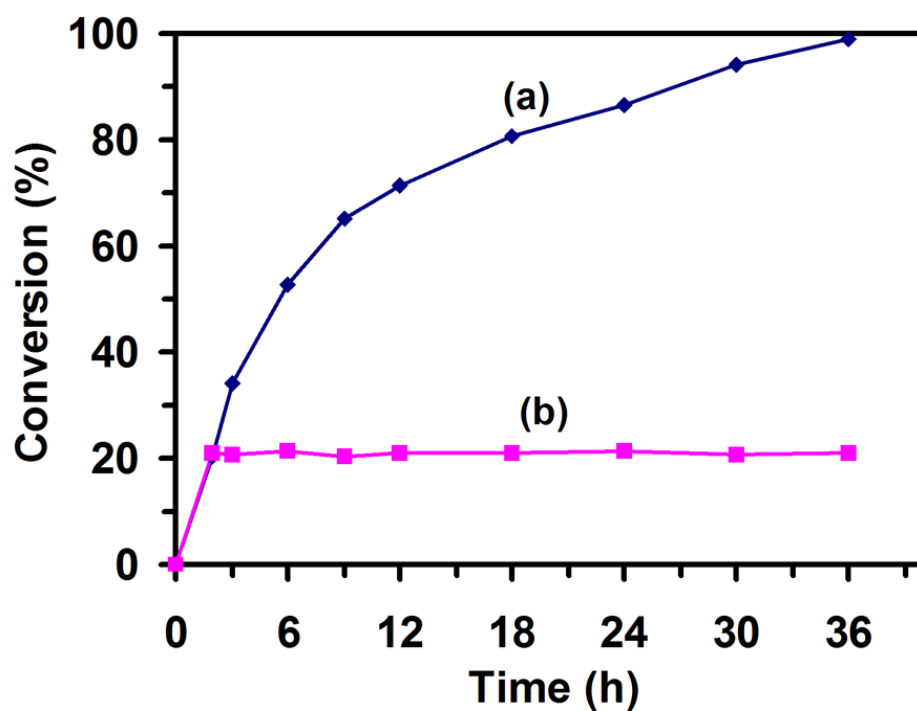


Figure S4. Activity profile for the cross-coupling of 4-iodoanisole with benzene. Reaction conditions: 4-iodoanisole (0.5 mmol), $KOt\text{-}Bu$ (3 equiv), MOF-253 (30 mol%), benzene (4 mL), 100 °C. (a) With catalyst and (b) with filtrate.

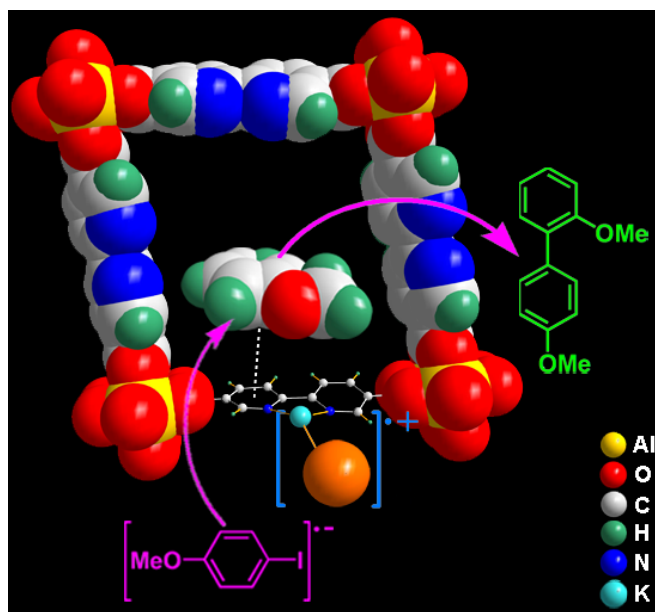


Figure S5. Plausible reaction mechanism of the arylation of anisole with 4-iodoanisole in the micropore of MOF-253. Orange ball represents the $-Ot\text{-Bu}$. Dotted line indicates the π,π -stacking interaction between the arene with the bpy ligand.

A plausible reaction mechanism of the arylation of anisole with 4-iodoanisole was formulated. As shown in Figure S5, the surface of MOF-253 is lined with open bpy coordination sites. In all the reports of transition-metal-free arylation reactions, aryl radical anions have been suggested as the key intermediates that are initiated by the bases and assisted by the organic molecules.²⁻⁴ Thus, we propose that the bpy sites might play a similar role to those reported organic ligands to facilitate the generation of aryl radicals (Figure S5). The aryl radical intermediates could be stabilized by the huge π -conjugated system of the MOF, consequently, the byproducts from the aryl halides may be remarkably suppressed. An analysis of the literature results indicates that electron-rich organomolecules also exhibited higher chemoselectivities than the relatively electron-deficient ligands.^{3b,c} Moreover, because of the fixed bpy moieties in the MOF, the formed aryl radicals are isolated with the bpy sites, and hence the homo-coupling byproducts can be significantly diminished. As a consequence, an excellent chemoselectivity to the cross-coupling products can be achieved with the MOF catalyst system.

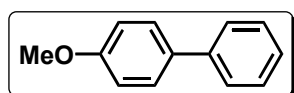
The significantly improved regioselectivities in comparison with the literature reports can be rationalized by considering the possible steric hindrance effects associated with the MOF structure. As measured by N₂ physical adsorption, the accessible pore size of the MOF-253 is *ca.* 8.0 Å (Figure S3). The KO*t*-Bu is believed to first interact with the bpy sites at the external surface of the MOF. The formation of complexed KO*t*-Bu at the surface will reduce the size of the windows, which makes diffusion through the MOF micropores more difficult. Therefore, it is proposed that the adsorption, activation, and reaction of the reactants possibly take place mostly on the external surfaces of the MOF crystals. We take the arylation of anisole as an example (Figure S5). Anisole molecules diffuse to the MOF surface and are embedded in the window most probably with the position that the aromatic ring is inward and almost parallel to the pore wall because of the steric hindrance (Table S4) as well as π,π -stacking interaction between the aromatic ring of anisole and the bpy ligand. The molecular orientations with dimensions larger than the pore size of the MOF will not be admitted into the pores.⁵ With such a configuration, the nucleophilic substitution to the *meta*- and *para*-positions will be greatly impeded, leading to a high ortho selectivity (Figure S5). The proposed mechanism can be applicable to explain the high regioselectivities in the arylation of the other substituted arenes investigated. This model is consistent with our experimental results that higher regioselectivities were obtained over the arenes with larger molecular dimensions (Table 3 of the text). Although further work is required to fully understand the mechanism, we believe that the electron configuration and steric hindrance of the micropores have played significant roles in achieving the excellent regioselectivities in the MOF catalytic system.

Reference

1. E. D. Bloch, D. Britt, C. Lee, C. J. Doonan, F. J. Uribe-Romo, H. Furukawa, J. R. Long, O. M. Yaghi, *J. Am. Chem. Soc.*, 2010, **132**, 14382.
2. S. Yanagisawa, K. Ueda, T. Taniguchi and K. Itami, *Org. Lett.*, 2008, **10**, 4673.
3. (a) W. Liu, H. Cao, H. Zhang, H. Zhang, K. H. Chung, C. He, H. Wang, F. Y. Kwong and A. Lei, *J. Am. Chem. Soc.*, 2010, **132**, 16737; (b) C.-L. Sun, H. Li, D.-G. Yu, M. Yu, X. Zhou, X.-Y. Lu, K.

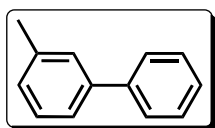
- Huang, S.-F. Zheng, B.-J. Li and Z.-J. Shi, *Nat. Chem.*, 2010, **2**, 1044; (c) E. Shirakawa, K.-i. Itoh, T. Higashino and T. Hayashi, *J. Am. Chem. Soc.*, 2010, **132**, 15537.
4. Y. Qiu, Y. Liu, K. Yang, W. Hong, Z. Li, Z. Wang, Z. Yao and S. Jiang, *Org. Lett.*, 2011, **13**, 3556.
5. C. E. Webster, R. S. Drago and M. C. Zerner, *J. Am. Chem. Soc.*, 1998, **120**, 5509.

3. Spectra Data for the Products



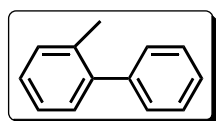
4-methoxybiphenyl (3a)

^1H NMR (400 MHz, CDCl_3): δ = 7.56-7.52 (m, 4H), 7.41 (t, J = 7.6 Hz, 2H), 7.30 (t, J = 7.4 Hz, 1H), 6.99-6.96 (m, 2H), 3.84 (s, 3H). ^{13}C NMR (100 MHz, CDCl_3): δ = 159.2, 140.9, 133.8, 128.7, 128.2, 126.7, 114.2, 55.4. GC-MS (EI): found: 184(M^+), calcd for $\text{C}_{13}\text{H}_{12}\text{O}$ (M^+): 184.09.



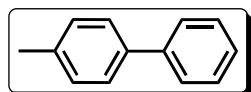
3-Methylbiphenyl (3b)

^1H NMR (400 MHz, CDCl_3): δ = 7.66 (d, J = 7.2 Hz, 2H), 7.46-7.52 (m, 4H), 7.40 (t, J = 7.4 Hz, 2H), 7.25 (d, J = 7.6 Hz, 1H), 2.50 (s, 3H). ^{13}C NMR (100 MHz, CDCl_3) δ = 141.4, 141.3, 138.3, 128.7, 128.0, 127.2, 124.3, 21.5. GC-MS (EI): found: 168(M^+), calcd for $\text{C}_{13}\text{H}_{12}$ (M^+): 168.09.



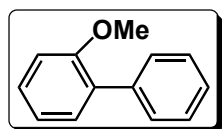
2-Methylbiphenyl (3c)

^1H NMR (400 MHz, CDCl_3): δ = 7.46-7.39 (m, 2H), 7.37-7.33 (m, 3H), 7.28-7.26 (m, 4H), 2.29 (s, 3H). ^{13}C NMR (100 MHz, CDCl_3): δ = 142.0, 135.4, 130.3, 129.8, 129.2, 128.1, 127.3, 126.8, 125.8, 20.5. GC-MS (EI): found: 168(M^+), calcd for $\text{C}_{13}\text{H}_{12}$ (M^+): 168.09.



4-Methylbiphenyl (3d)

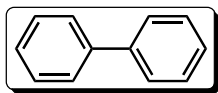
^1H NMR (400 MHz, CDCl_3): δ = 7.57 (d, J = 7.2 Hz, 2H), 7.48 (d, J = 8.0 Hz, 2H), 7.41 (t, J = 7.6 Hz, 2H), 7.31 (t, J = 7.4 Hz, 1H), 7.23 (d, J = 7.6 Hz, 2H), 2.38 (s, 3H). ^{13}C NMR (100 MHz, CDCl_3): δ = 141.2, 138.4, 137.0, 129.5, 128.7, 127.0, 21.1. GC-MS (EI): found: 168(M^+), calcd for $\text{C}_{13}\text{H}_{12}$ (M^+): 168.09.



2-methoxybiphenyl (3e)

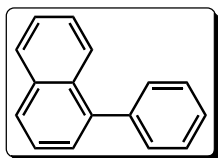
^1H NMR (400 MHz, CDCl_3): δ = 7.58-7.56 (m, 2H), 7.39 (t, J = 7.6 Hz, 2H), 7.32-7.27 (m, 3H), 7.03-6.94 (m, 2H), 3.77 (s, 3H). ^{13}C NMR (100 MHz, CDCl_3): δ = 156.5, 138.6, 130.8, 129.6, 128.6, 128.0, 126.9, 120.8, 111.3, 55.6. GC-MS (EI): found: 184(M^+), calcd for $\text{C}_{13}\text{H}_{12}\text{O}$ (M^+): 184.09.

Biphenyl (3f)



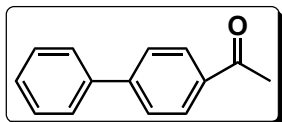
^1H NMR (400 MHz, CDCl_3): $\delta = 7.69$ (d, $J = 7.2$ Hz, 4H), 7.53 (t, $J = 7.4$ Hz, 4H), 7.44 (t, $J = 7.4$ Hz, 2H). ^{13}C NMR (100 MHz, CDCl_3): $\delta = 141.3, 128.8, 127.3, 127.2$. GC-MS (EI): found: 154(M^+), calcd for $\text{C}_{12}\text{H}_{10}$ (M^+): 154.08.

1-Phenylnaphthalene (3g)



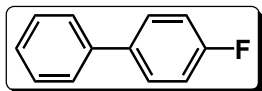
^1H NMR (400 MHz, CDCl_3): $\delta = 7.95$ -7.88 (m, 3H), 7.62-7.51 (m, 6H), 7.51-7.43 (m, 3H). ^{13}C NMR (100 MHz, CDCl_3): $\delta = 140.8, 140.3, 133.8, 131.7, 130.1, 128.3, 127.7, 127.3, 127.0, 126.1, 125.8, 125.4$. GC-MS (EI): found: 204(M^+), calcd for $\text{C}_{16}\text{H}_{12}$ (M^+): 204.09.

4-Acetyl-biphenyl (3h)



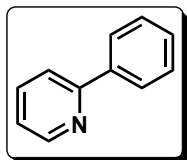
^1H NMR (400 MHz, CDCl_3): $\delta = 8.04$ (d, $J = 8.4$ Hz, 2H), 7.69 (d, $J = 8.4$ Hz, 2H), 7.67-7.59 (m, 2H), 7.53-7.39 (m, 3H), 2.64 (s, 3H). ^{13}C NMR (100 MHz, CDCl_3): $\delta = 197.8, 145.8, 139.9, 135.9, 129.0, 128.9, 128.2, 127.3, 127.2, 26.7$. GC-MS (EI): found: 196(M^+), calcd for $\text{C}_{14}\text{H}_{12}\text{O}$ (M^+): 196.09.

4-Fluorobiphenyl (3i)



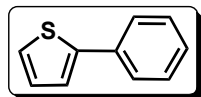
^1H NMR (400 MHz, CDCl_3): $\delta = 7.61$ -7.58 (m, 4H), 7.49 (t, $J = 7.6$ Hz, 2H), 7.40 (t, $J = 7.4$ Hz, 1H), 7.18 (t, $J = 8.8$ Hz, 2H). ^{13}C NMR (100 MHz, CDCl_3): $\delta = 163.7, 161.3, 140.3, 137.4, 137.3, 128.9, 128.7, 128.6, 127.3, 127.0, 115.7, 115.5$. GC-MS (EI): found: 172(M^+), calcd for $\text{C}_{12}\text{H}_9\text{F}$ (M^+): 172.07.

2-phenylpyridine(3j)



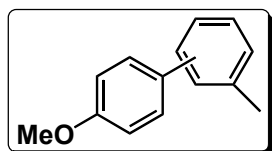
^1H NMR (400 MHz, CDCl_3): $\delta = 8.69$ (d, $J = 4.8$ Hz, 1H), 7.99 (d, $J = 7.2$ Hz, 2H), 7.79 – 7.68 (m, 2H), 7.47 (t, $J = 7.2$ Hz, 2H), 7.41 (t, $J = 6.8$ Hz, 1H), 7.26 – 7.18 (m, 1H). ^{13}C NMR (100 MHz, CDCl_3): $\delta = 157.5, 149.7, 139.4, 136.7, 129.0, 128.7, 126.9, 122.1, 120.6$. GC-MS (EI): found: 155(M^+), calcd for $\text{C}_{11}\text{H}_9\text{N}$ (M^+): 155.20.

2-phenylthiophene(3k)



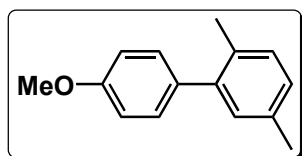
^1H NMR (400 MHz, CDCl_3): $\delta = 7.64\text{--}7.53$ (m, 2H), 7.34 (t, $J = 7.6$ Hz, 2H), 7.29–7.19(m, 3H), 7.03(dd, $J = 5.0$ Hz, 1H). ^{13}C NMR (100 MHz, CDCl_3): $\delta = 144.5, 134.5, 129.0, 128.1, 127.5, 126.0, 124.9, 123.2$. GC-MS (EI): found: 160(M^+), calcd for $\text{C}_{10}\text{H}_8\text{S}$ (M^+): 160.24.

Mixture of 4'-methoxy-2-methylbiphenyl, 4'-methoxy-3-methylbiphenyl, 4'-methoxy-4-methylbiphenyl (3l)



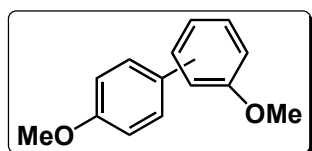
^1H NMR (400 MHz, CDCl_3): $\delta = 7.54\text{--}7.22$ (m, 6H), 6.96–6.94 (m, 2H), 3.85 (s, 3H), 2.41–2.28 (m, 3H). GC-MS (EI): found: 198(M^+), calcd for $\text{C}_{14}\text{H}_{14}\text{O}$ (M^+): 198.10.

2, 5-dimethyl-4'-methoxybiphenyl (3m)



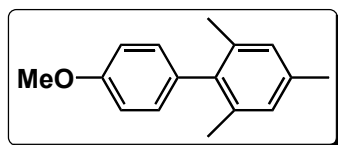
^1H NMR (400 MHz, CDCl_3): $\delta = 7.24$ (d, $J = 8.0$ Hz, 2H), 7.14 (d, $J = 8.4$ Hz, 1H), 7.04 (d, $J = 6.4$ Hz, 2H), 6.94 (d, $J = 8.4$ Hz, 2H), 3.84 (s, 3H), 2.33 (s, 3H), 2.23 (s, 3H). ^{13}C NMR (100 MHz, CDCl_3): $\delta = 158.5, 141.4, 135.2, 134.5, 132.3, 130.7, 130.2, 127.7, 113.5, 55.3, 20.9, 20.1$. GC-MS (EI): found: 212(M^+), calcd for $\text{C}_{15}\text{H}_{16}\text{O}$ (M^+): 212.12.

Mixture of 2,4'-dimethoxybiphenyl, 3,4'-dimethoxybiphenyl, 4, 4'-dimethoxybiphenyl (3n)



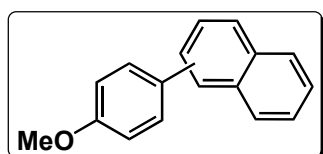
^1H NMR (400 MHz, CDCl_3): $\delta = 7.53\text{--}7.45$ (m, 2H), 7.30–7.23 (m, 2H), 6.02–7.93 (m, 4H), 3.86–3.79 (m, 6H). GC-MS (EI): found: 214(M^+), calcd for $\text{C}_{14}\text{H}_{14}\text{O}_2$ (M^+):214.10.

4'-methoxy-2, 4, 6-trimethylbiphenyl (3o)

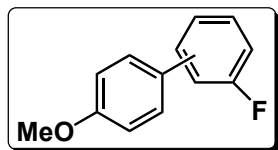


^1H NMR (400 MHz, CDCl_3): $\delta = 7.04$ (d, $J = 8.4$ Hz, 2H), 7.00–6.88 (m, 4H), 3.84 (s, 3H), 2.32 (s, 3H), 2.01 (s, 6H). ^{13}C NMR (100 MHz, CDCl_3): $\delta = 158.2, 138.7, 136.5, 133.5, 130.4, 128.1, 113.8, 55.2, 21.0, 20.8$. GC-MS (EI): found: 226(M^+), calcd for $\text{C}_{16}\text{H}_{18}\text{O}$ (M^+): 226.14.

Mixture of 1-(4-anisyl)-naphthalene, 2-(4-anisyl)-naphthalene (3p)

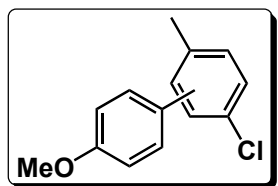


^1H NMR (400 MHz, CDCl_3): δ = 7.90-7.56 (m, 4H), 7.44-7.31 (m, 5H), 6.96-6.92 (m, 2H), 3.80-3.78 (d, J = 8.6 Hz, 3H). GC-MS (EI): found: 234(M^+), calcd for $\text{C}_{17}\text{H}_{14}\text{O}$ (M^+): 234.10.



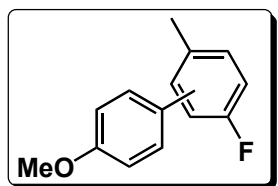
Mixture of 2-fluoro-4'-methoxybiphenyl, 3-fluoro-4'-methoxybiphenyl, 4-fluoro-4'-methoxybiphenyl (3q)

^1H NMR (400 MHz, CDCl_3) δ 7.55-6.87 (m, 8H), 3.84 (s, 3H). GC-MS (EI): found: 202(M^+), calcd for $\text{C}_{13}\text{H}_{11}\text{FO}$ (M^+): 202.08.



Mixture of 4'-methoxy-2-chloro-5-methylbiphenyl, 4'-methoxy-2-methyl-5-chlorobiphenyl (3r)

^1H NMR (400 MHz, CDCl_3): δ =7.52-6.79 (m, 8H), 3.84 (s, 3H), 2.34-2.22 (d, 3H). GC-MS (EI): found: 232 (M^+), calcd for $\text{C}_{14}\text{H}_{13}\text{ClO}$ (M^+): 232.07.



Mixture of 4'-methoxy-2-fluoro-5-methylbiphenyl, 4'-methoxy-2-methyl-5-fluorobiphenyl (3s)

^1H NMR (400 MHz, CDCl_3) δ 7.24-7.16 (m, 3H), 7.02-6.90 (m, 4H), 3.84 (s, 3H), 2.35-2.22 (d, 3H). GC-MS (EI): found: 216 (M^+), calcd for $\text{C}_{14}\text{H}_{13}\text{FO}$ (M^+): 216.10.

4. ^1H NMR and ^{13}C NMR Spectra of products

